

## Impurity modes and effect of clustering in diluted semiconductor alloys

Andrei Postnikov, Olivier Pagès, Ayoub Nassour and Joseph Hugel

LPMD, Paul Verlaine University – Metz, 1 Bd Arago, F-57078 Metz, France

postnikov@univ-metz.fr

The variation of TO zone-center vibration spectra with concentration in mixed zincblende-type semiconductors can be understood within a paradigm of unified “one bond – two modes” approach, which has been recently outlined as a rather general concept,<sup>1</sup> and emerges from a number of previous experimental and theoretical studies.<sup>2,3</sup> The crucial issue is that the vibration frequency, associated with a certain cation-anion bond, depends on the length of the latter, and the bond length, in its turn, depends not only on the average alloy concentration, but on local variations of it. In an (A,B)C substitutional alloy, the A–C bond length differ in A-rich and A-poor regions, yielding a splitting of the A–C vibration frequency. Such splittings can be measured and reproduced in first-principles calculations.

An analysis of vibration spectra helps to get an insight into the structural short-range (clustering) and long-range (formation of extended chains of certain cation-anion pairs and other structural motives at the mesoscopic scale) tendencies. For this however, one needs first-principles benchmark calculations for representative model systems (see, e.g., Ref. 4 for the ZnSe–BeSe alloys). The simplest yet important result from first-principles calculations is a prediction of how the impurity phonon mode evolves as isolated (distant) impurities get clustered.

In the present contribution, we outline the results of first-principles calculations of phonon frequencies and vibration patterns, in the dilution limits of several mixed semiconductor alloys,  $\text{Be}_x\text{Zn}_{1-x}\text{Se}$ ,  $\text{Ga}_x\text{In}_{1-x}\text{As}$  and  $\text{Ga}_x\text{In}_{1-x}\text{P}$ . The calculations have been done by the SIESTA method<sup>5</sup> for cubic 64-atom supercells, with one or two cation atoms substituted by impurity species, that corresponds to impurity contents of 3% and 6%, respectively. The initial unconstrained structure relaxation for each supercell chosen was followed by a calculation of phonons by finite displacement technique. Each of the atoms in the supercell were subject to 6 consecutive small cartesian displacements, and the forces induced on all atoms in the supercell resulted in corresponding force constants.

The analysis of results is the simplest for  $\text{Be}_x\text{Zn}_{1-x}\text{Se}$ , a system with large contrast in masses and elastic properties between its parent compounds, that leads to a big separation between Zn-related and Be-related phonon modes (see Ref. 4 for details). Fig. 1 shows the phonon

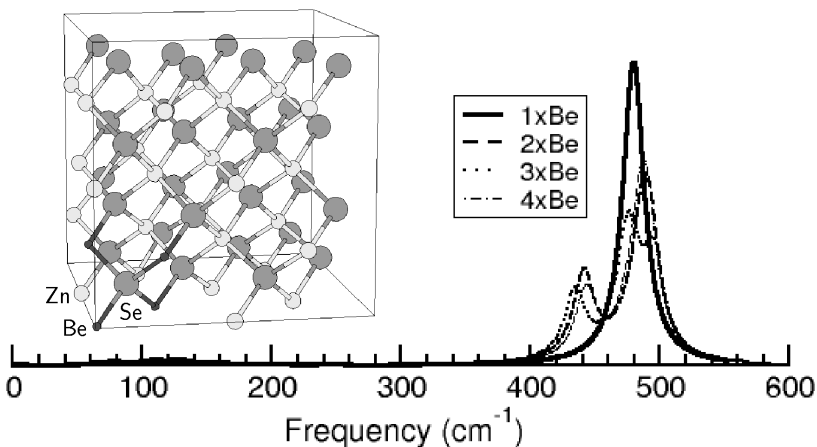


Fig. 1. Phonon density of states of Be, after first-principles calculations for  $\text{Be}_n\text{Zn}_{32-n}\text{Se}_{32}$  supercells, with 1,..4 Be cations neighbouring the same Se anion. The supercell for  $n=4$  is shown in the inset.

density of states for Be, for the cases of single impurity and impurity pair (both Be atoms being neighbours to the same Se). Moreover, the cases of three and four Be atoms grouping around the same Se are considered for this system (the  $\text{Be}_4\text{Zn}_{28}\text{Se}_{32}$  supercell is shown in the inset to Fig. 1). One clearly sees that the single vibration peak of an isolated impurity (a nearly triply degenerate mode of Be in tetrahedral  $\text{Se}_4$  cage) splits into two peaks, separated by  $\sim 40\text{ cm}^{-1}$ , as another Be impurity is introduced. The origin for this splitting is a diversification of Be–Se bond lengths, as two Be share the same Se atom. Namely, the bonds to outer Se atoms of the Be–Se–Be cluster can be much more efficiently shortened in the course of structure relaxation than the bonds to the central Se. Shorter bonds imply larger force constants and hence higher vibration frequency (again, see Ref. 4 for a more detailed discussion). It is noteworthy that an addition of further Be atoms as neighbors to the central Se brings in some additional structure, but leaves in place the initial major splitting into two big groups of peaks, those characterizing a “Be-poor” environment (at  $\sim 480\text{ cm}^{-1}$ ) and “Be-rich” environment (at  $\sim 440\text{ cm}^{-1}$ ).

In the following we compare this initial splitting of single-impurity mode into a doublet of interacting-impurities modes with the experimentally observed onset of the “1-bond $\rightarrow$ 2-mode” behaviour, discussed previously.<sup>1–4</sup> Notably, the impurity mode at  $\sim 440\text{ cm}^{-1}$  in the  $x\rightarrow 0$  limit of  $\text{Be}_x\text{Zn}_{1-x}\text{Se}$  develops into two branches, at  $\sim 450\text{ cm}^{-1}$  and  $\sim 410\text{ cm}^{-1}$ , at small values of  $x$  – see Fig. 1 of Ref. 6. It should be noted (and was already discussed in Ref. 4) that the absolute values frequencies are shifted upwards in our calculation, with respect to their experiment values, due to a slight overbinding caused by the local density approximation to the exchange-correlation. However, the frequency difference between the single-impurity and

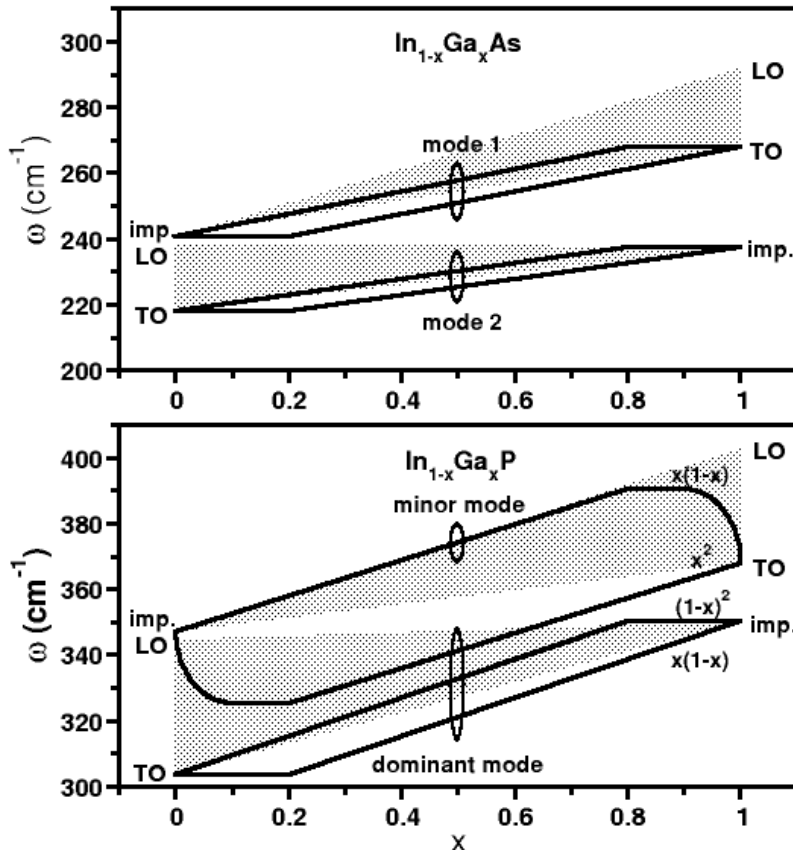


Fig. 2. Simplified 1-bond $\rightarrow$ 2-mode TO (thick lines) percolation schemes of (InGa)As and (InGa)P. The generic fraction of bonds corresponding to each TO branch is indicated in the bottom panel. The bond-related optical bands simply obtained by linear convergence of the parent TO and LO frequencies onto the related impurity frequencies are shown as shaded areas.

double-impurity modes is fairly reproduced.

The general behaviour of phonon modes depending on the Be concentration, “streamlining” the experimental details from Fig. 1 of Ref. 6, is shown and discussed in Ref. 7. It was argued<sup>1</sup> that the similar schema holds for other semiconductor alloys, even if the position of branches and their splittings may differ. Fig. 2 reproduces a part of experimental findings schematically presented in Fig. 4 of Ref. 1. Below we discuss the *ab initio* predictions of the single impurity vs. impurity pair -related phonon behaviour for (Ga,In)As and (Ga,In)P alloys.

For the identification of zone-center phonon modes it is convenient to refer to  $\mathbf{q}$ -projected phonon density of states (PhDOS), which can be introduced as

$$I_{\aleph}(\omega, \mathbf{q}) = \sum_i \left| \sum_{\alpha \in \aleph} A_i^\alpha(\omega) \exp(\mathbf{q}\mathbf{R}_\alpha) \right|^2$$

where  $A_i^\alpha(\omega)$  is phonon eigenvector for atom  $\alpha$  at frequency  $\omega$ , and  $\aleph$  – an arbitrarily chosen group of atoms (say, those of a given chemical species). The  $\mathbf{q}=0$  -projected PhDOS of a host atom selects the zone-center vibrations which contribute to the Raman spectra, like e.g. a TO-mode of bulk InAs at  $\sim 220 \text{ cm}^{-1}$  is prominent in the PhDOS of In in Fig. 3. For Ga, which is a single impurity, the  $\mathbf{q}$ -projected PhDOS coincides with the full vibrational density of states and spans the whole interval of frequencies, from 0 to  $250 \text{ cm}^{-1}$ . Yet, not all of these modes are zone-center-like, if one takes into account the vibration of the As sublattice. A direct inspection of different vibration patterns reveals, as genuine zone-center vibration modes, a triplet at  $246 \text{ cm}^{-1}$ . In the  $\mathbf{q}=0$  -projected PhDOS of In (Fig. 3) and of As (not shown, as it is practically identical with that of In), a split-off peak on the high-frequency side of the main TO line does also reveal the presence of this impurity mode, which is an in-phase vibration of Ga impurity with the In sublattice, in counter-phase to the As sublattice.

Turning to the analysis of impurity pair, we find several modes, which correspond to in-phase vibration of Ga atoms with the In sublattice and in counter-phase with the As sublattice. These modes span the range of  $248\text{--}251 \text{ cm}^{-1}$ .

On the opposite end of the concentration scale, the vibration of isolated In in GaAs, as a heavy impurity, mixes up with a “continuum” of bulk modes. Still, the major impurity modes can be identified near  $238 \text{ cm}^{-1}$ . The impurity pairs vibrate in phase between themselves and with the cation sublattice in the region  $235\text{--}241 \text{ cm}^{-1}$ , again in agreement with the measured vibration zone-center frequencies shown in Fig. 2. The first-principles calculations yield therefore, on both low-concentration sides of the concentration scale of (Ga,In)As, the zero splitting from single-impurity frequency to the two-mode regime. This is consistent with experimental observations summarized in Fig. 2.

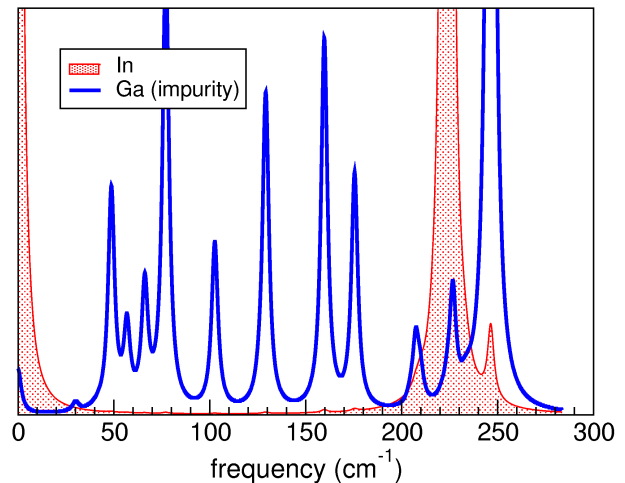


Fig. 3.  $\mathbf{q}=0$  -projected phonon density of states of Ga and In in  $\text{Ga}_1\text{In}_{31}\text{As}_{32}$  supercell.

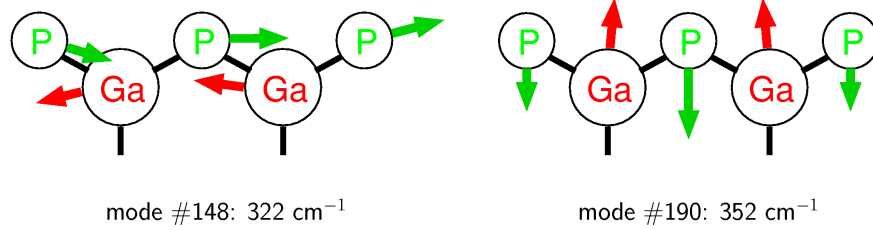


Fig. 4. Two in-phase vibrations of Ga impurity pair with strong zone-center contribution in the vibrations of the anion sublattice, according to calculations in the Ga<sub>2</sub>In<sub>30</sub>P<sub>32</sub> supercell.

For (Ga,In)P the situation is different. In the experiment, the two-mode regime which sets on under the Ga doping is characterized by a quite large splitting (of  $\sim 20$  cm<sup>-1</sup>) between the two Ga–P modes. Indeed we could recover this splitting in the calculation. Fig. 4 shows the vibration patterns of two maximally split in-phase double-impurity modes. The softest of these modes (322 cm<sup>-1</sup>) is a “longitudinal” displacement of two Ga atoms against the P atom in between, making one Ga–P bond longer at the expense of the other. The hardest mode (352 cm<sup>-1</sup>) involves a different “two Ga against P” displacement, which lies in the Ga–P–Ga plane as in the first case, but occurs in the perpendicular direction, bending the Ga–P–Ga angle. This vibration is slightly harder than the single-Ga impurity mode whose calculated frequency is 350 cm<sup>-1</sup>. Taken together, the arrangement of calculated vibration modes agrees well with the experimental observations summarized in Fig. 2 (up to a small systematic blue shift of calculated frequencies with respect to experiment, discussed above).

On the Ga-rich side of the schema in the lower panel of Fig. 2, no noticeable splitting was detected in experiment, and again this is consistent with the calculation: single-In impurity modes at 360 cm<sup>-1</sup> develop, on addition of a second In impurity, into a bunch of two-impurity modes, which are confined in a quite narrow range, 357 to 362 cm<sup>-1</sup>.

Summarizing, we have shown, on discussing impurity limits in three semiconductor alloys, how the important parameters of the concentration–frequency diagram for mixed semiconductors discussed in Ref. 1, the single impurity frequencies and their initial splitting on the onset of one-bond→two-mode behaviour can be extracted from first-principles calculations.

We acknowledge the access to the calculation resources at the CINES in Montpellier (projet N° pli2623).

1. O. Pagès, M. Kassem, A. Chafi, A. Nassour, S. Doyen and A. V. Postnikov, <http://arxiv.org/abs/0709.0930>
2. O. Pagès, M. Ajjoun, D. Bormann, C. Chauvet, E. Tournié and J. P. Faurie, Phys. Rev. B **65**, 035213 (2002).
3. O. Pagès, T. Tite, K. Kim, P.A. Graf, O. Maksimov and M.C. Tamargo, J.Phys.: Condens.Matter **18**, 577 (2006).
4. A.V. Postnikov, O. Pagès and J. Hugel, Phys. Rev. B **71**, 115206 (2005).
5. <http://www.uam.es/siesta>; P. Ordejon, E. Artacho and J. M. Soler, Phys. Rev. B **53**, R10441 (1996); J.M. Soler, E. Artacho, J.D. Gale, A. García, J. Junquera, P. Ordejón, and D. Sánchez-Portal, J. Phys.: Condens. Matt. **14**, 2745 (2002).
6. O. Pagès, M. Ajjoun, T. Tite, D. Bormann, E. Tournié and K.C. Rustagi, Phys. Rev. B **70**, 155319 (2004).
7. O. Pagès, A. V. Postnikov, A. Chafi, D. Bormann, P. Simon, F. Firszt, W. Paszkowicz and E. Tournié, cond-mat/0610682.